A multimode thermooptic beam steering switch

Jonathan Rogers, Changbao Ma, Makarand Paranjape, Edward Van Keuren*

Department of Physics
Georgetown University
Washington, DC 20057

ABSTRACT

Thermooptic switches are viable options for rapidly and reliably switching and routing optical signals in planar lightwave circuits. We present modeling and fabrication of a thermooptic switch made of the polymer SU-8, an epoxy resin commonly used as a MEMS structural material. SU-8 is a good candidate material for use in planar waveguides due to its high refractive index, good transmission properties in the visible and infrared, and excellent thermal and mechanical stability. Furthermore, it has great advantages in fabrication since it is used as a negative photoresist, and so can be patterned directly using photolithography. Light is guided by a refractive index gradient generated by embedded MEMS microheaters, which activate the thermal nonlinearity of the polymer. The thermooptic change in refractive index imparts an inhomogeneous phase shift to the beam in the waveguide, which guides the input into one of two or more outputs. The switch design and operation parameters have been optimized using simulations of the thermal profile using finite element modeling and of the optical propagation using the beam propagation method.

Keywords: Thermooptic switch, Beam Propagation Method, Planar Lightwave Circuits

1. INTRODUCTION

Photonic switching components are critical elements of current optical telecommunications systems, most of which utilize wavelength division multiplexing (WDM) to achieve high bandwidths. WDM enables much higher information content to be transmitted than time division multiplexing, but requires components with low loss and flat wavelength response (all wavelengths have identical transmission through the device and are switched with the same input power).[1]

Recently, the scale for photonic communications has moved to shorter distances, from long-distance telecommunications to optical fiber to the home. This trend is likely to extend to interboard and interchip communications in computers,[2] which is particularly critical as limitations on computing speed are becoming more dependent on communications bottlenecks between chips, for example memory and CPU. Optical backplanes and interconnects are some of the technologies being implemented in order to address these problems.[3] Planar lightwave circuits (PLCs), integrated photonics devices incorporating waveguides and additional passive and active elements for signal processing and routing, are expected to play important roles in easing these bottlenecks, and are being developed by numerous groups worldwide.[4]

In principle, light propagation through PLCs and other photonic devices is governed by the variation of the phase of the light as a function of the spatial coordinates of the device. This phase is related to the material through the real part of the complex refractive index, and waveguiding is achieved by variations in the refractive index. For example, in passive waveguiding devices such as optical fibers, light is confined to a high index medium surrounded by one with a lower index. Phase may also be used for active control of light, for example by changing the refractive index in one arm of a Mach-Zehnder interferometer in order to change the degree of interference of the recombined beams and so switch the total output of the device. This change in the refractive index of the active switching material can be achieved by various phenomena, for example, second order nonlinear optical effects,[5] where static electric fields are

* vankeu@physics.georgetown.edu; phone +1-202-687-5982

Optoelectronic Devices: Physics, Fabrication, and Application III, edited by Joachim Piprek, Jian Jim Wang,
Proceedings of SPIE Vol. 6368, 636815, (2006) · 0277-786X/06/$15 · doi: 10.1117/12.686226

used to invoke changes in refractive indices. Other examples of devices using spatial variation in refractive index to control light include interference filters, dielectric mirrors and photonic crystals.

These examples all represent devices using homogeneous changes to the refractive index to enable control of beam propagation. We are developing actively controllable devices based on waveguiding using variable index gradients. These devices use the full possibilities of inhomogeneous refractive index profiles to control the wavefront of the propagating beams, thereby enabling devices such as directional couplers, switches and routers. As in graded index fibers, light guiding is achieved by continuous spatial variations in the refractive index. However, these gradients are generated though nonlinear optical processes, allowing active control of beam propagation by external controls such as temperature or electric field.

The development of a device using this concept is presented here: a simple directional coupler shown schematically in Figure 1. The switch operates using the thermooptic effect, in which a change in temperature causes a change in the refractive index of a material. In the device, light is inserted into a waveguide with a square or rectangular cross section, and propagates to a Y-branch, where it splits into two equal parts. Near the branch point, a set of microheaters are embedded below the waveguide on either side. The heaters are symmetrically positioned on each side in order to locally increase the temperature on one side or the other of the waveguide. When current is applied to one of these heaters, the local temperature increase on one side of the waveguide induces a gradient in the refractive index perpendicular to the direction of the light beam. The light will be steered towards regions of higher

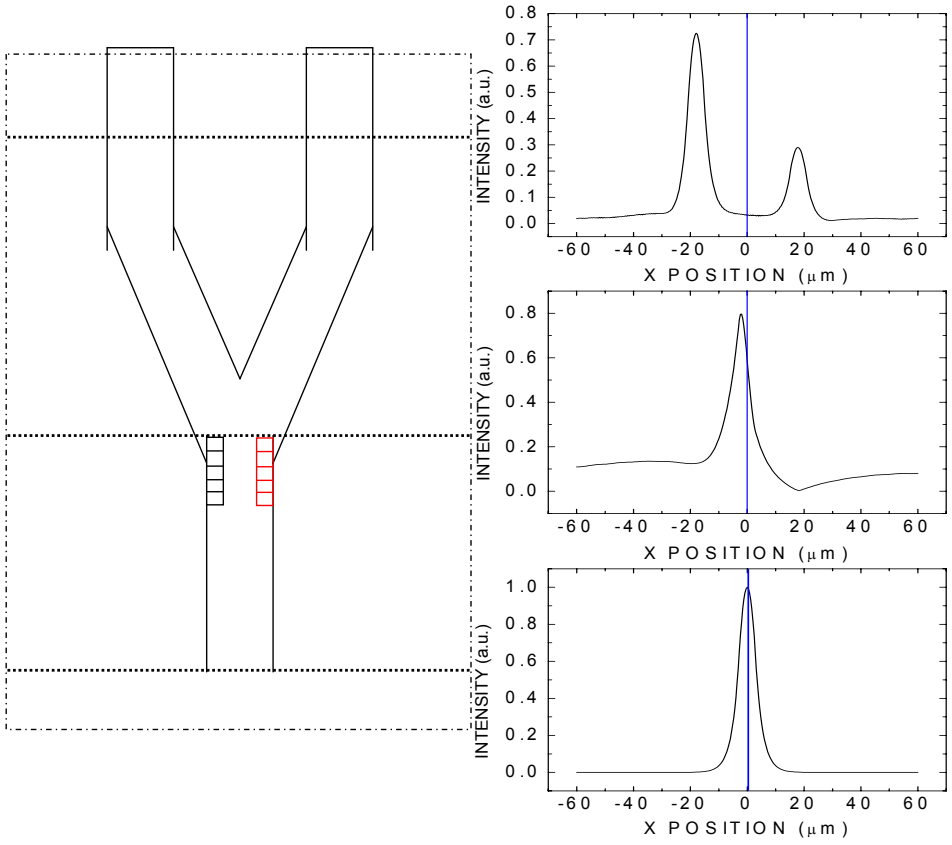

Figure 1: Top view of switch structure (left). The beam profile at each of the horizontal dotted lines are shown on the right when a linear refractive index gradient with magnitude 9×10^{-3} is generated in the waveguide near the heaters. The heater on the right hand side is active, resulting in a decrease in the refractive index on this side, which guides the light to the left branch.

refractive index into one or the other of the branches. As a result, the device functions as an electrically addressable router; by applying power to one of the heaters, the light preferentially enters one of the branches.

The requirements for the material used for our device are similar to those for other PLC components, in particular, it must have good optical quality (low absorption and scattering). Typical materials used for optical waveguides and PLC components include silica glass[6] and polymers.[7] In addition, for PLCs the material must be able to be easily fabricated and integrated into existing semiconductor circuit technology. Finally, the active area of our device needs to have a large thermooptic coefficient, or change in refractive index per change in temperature. Besides the ease in processing and ability to vary the chemical structure, polymers have a particular advantage as thermooptic materials.[8] due to their typically high values of thermooptic coefficient. They display large changes in refractive index with increasing temperature, usually linked to changes in the density of the material. This enables a sufficiently large index change to be achieved for low input power.

We have implemented the design described above using the epoxy resin SU-8, which has recently been shown to be an effective waveguide material.[9] It is commonly used as a high aspect ratio mold or as a structural material in MEMS fabrication, and can be directly patterned using standard UV photolithography. SU-8 is a good candidate material for use in planar waveguides due to its high refractive index, good transmission properties in the visible and near infrared wavelength regions, and excellent thermal and mechanical stability. The ability to directly pattern SU-8 means MEMS fabrication techniques can be used to create both waveguide and active switching element from a single polymer material.

The device principle has advantages of simplicity and ease of fabrication. Its application is targeted to datacom and board-level optical interconnects, where ease of integration with existing technology is as important as low power operation and good switching speeds. In addition, the problems with absorption of polymeric materials in the IR telecom bands (wavelengths > 1000 nm) is no longer an issue at the shorter datacom wavelengths below 1000 nm. The device has direct advantages compared to other technologies, such as flat wavelength response, a simple fabrication method and robust operation. More importantly, the same principle can easily be applied to the creation of other novel devices for controlling optical pulses in PLCs, for example, 1-N couplers and reconfigurable interconnects. Other methods of generating index gradients may also applied, for example by using an electric field gradient with an electrooptic material.

Here we report on our initial work in the development of the switch, including simulation and optimization of the device geometry, fabrication, and initial characterization.

2. DEVICE DESIGN AND FABRICATION

2.1. Switch material and design

Besides the advantages of direct write fabrication with SU-8, its optical properties are excellent for waveguide applications. Figure 2 shows a VIS/NIR absorption spectrum of an SU-8 film, indicating relatively low absorption and flat response below about 1100 nm down to the UV. No strong absorption bands appear in the regions near the datacom bands at 850 or 1310 nm, indicating that the material would be suitable for low-loss waveguides at these wavelengths. Ellipsometry measurements of a number of thin films at wavelength 633 nm gave an average refractive index of 1.54. While the photostability has not been measured, the fully cross-linked (exposed and baked) material is transparent above 400 nm, and the high degradation temperature (~380 °C) suggests that this will not be a serious problem

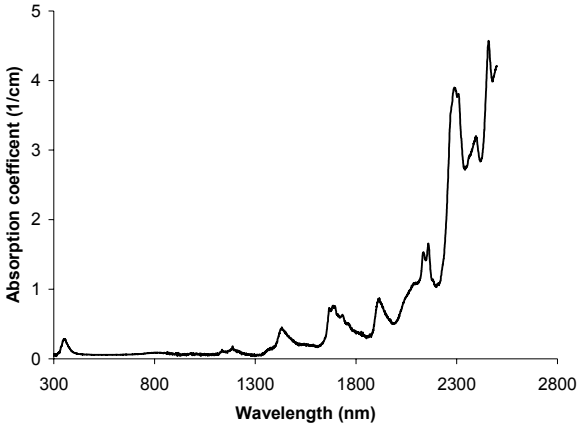

Figure 2: Absorption spectrum of SU-8.

With a target application in board level interconnects, our switch has been designed to be multimode, since source and detector elements have typical sizes on the order of 10's of microns across,[10] and the short distances mean that modal dispersion is not a major problem. While thermooptic beam steering is straightforward in single mode waveguides,[11] it is more complicated in multimode structure, since a given index gradient will have varying effects on the different modes, and the total beam may not be efficiently steered or switched.

The initial devices were based on quite large multimode waveguides (~100 μm core width), both for the low cost of fabrication, since the mask resolution was less critical, and because of the ease of coupling light in and out of the waveguides. However, this presents problems both in simulation, described in the following section, and in the need for higher power to achieve the temperature gradient over large areas and to switch all the multiple modes in the waveguide. In order to resolve these problems, a second generation device with smaller waveguide cores (16 × 16 μm^2) was designed, simulated and fabricated. This switch was still multimode, enabling an investigation of the effects of the inhomogeneous index profile on the multimode beam propagation.

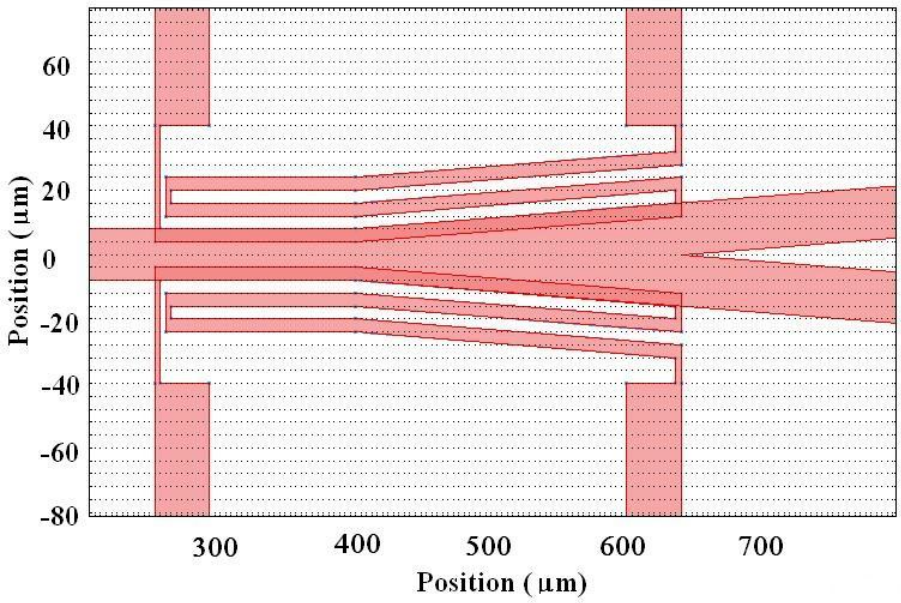

Figure 3: Geometry of the Y-branch.

The structure of the Y-branch is shown in figure 3. The SU-8 waveguide is on top of a glass substrate, with microheaters placed underneath near the branch point. The glass served as the lower cladding, while the sides and upper cladding was air. The heater elements are 5 μm wide, with a serpentine structure running along the waveguides. Simulations of the temperature profile indicated that this geometry would provide a high gradient across the waveguides.[12] The models also indicated that the heater placement with respect to the waveguide branch is critical for effective switching, in particular for multimode structures. The heaters need to cover the entire branching section, otherwise, the wave profile will be shifted towards one of the output branches, but will redistribute before being completely coupled into this branch, resulting in a decrease in the ratio of power between the two branches. It was also found that the distance of the heaters from the waveguides is important for the efficiency. The steepest temperature (and refractive index) gradient across the waveguide was obtained with the heaters approximately 1/3 beneath the core, and the remainder under the cladding.

The other critical aspect of the geometry is the angle of the Y-branch. Smaller angles reduce the total insertion loss of the switch, since the light is more effectively coupled into the two branches (less loss due to the change in the

waveguide orientation at the branching point). However, smaller angles also requires longer effective length of the branch region, and longer microheaters. Varying the branch angle between 1 and 4 degrees in both simulations and fabricated devices was carried out in order to determine optimal values.

2.2. Simulations

Computer modeling of the functioning of the switch was performed in order to test the principle and aid in the initial optimization of the device geometry. The modeling of the optical signal was done using the beam propagation method. We implemented the finite difference beam propagation method [13, 14] and used it to model the propagation in single- and multimode channel waveguides containing refractive index gradients.[11] In the model, the optical electric field is discretized in the plane perpendicular to the direction of motion, and a matrix propagator is used iteratively to find the evolution of the wave as it travels along the waveguide. This algorithm allows one to easily incorporate an inhomogeneous refractive index profile similar to the type we will generate from the microheater. The refractive index profile, determined both theoretically and experimentally from temperature and nonlinear optical characterization, will be an input into the model of the propagation of optical pulses through the device.

We modeled the temperature profiles in the active areas of the switch using the commercial finite element modeling package FEMLAB™ (Comsol). Using this software, preliminary simulations of temperature distributions, gradients and fluxes were performed. FEMLAB uses a heat balance equation, derived from the principle of conservation of energy, to find a nodal solution for each finite element that defines the device structure. With its multiphysics features, combinations of physical effects can be simultaneously modeled, either using built-in application modes by directly specifying physical parameters rather than partial differential equations, or by creating custom equations with equation-based modeling. Based on the temperature distribution and the thermooptic coefficient of the materials, the refractive index change due to thermooptic effects can be determined.

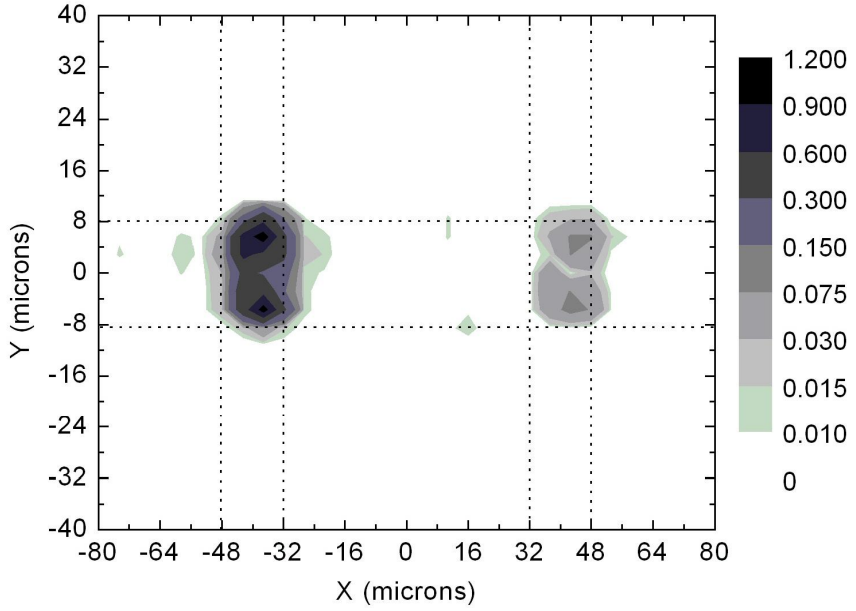

Figure 4: Beam propagation simulations results, showing the beam profiles looking into the two output branches of the switch for an applied power of 70 mW to the microheater on the right hand side of the branch. The plot represented the normalized output optical power at 1 ms after application of the heater current.

Figure 4 shows the simulated output of the two branches of the switch for an applied power of 70 mW to one of the heaters, at 1 ms after the application of the heat pulse. These results are for a switch with a branching angle of 3.8º and for a thermooptic coefficient of 10^{-4}/K. The ratio of the optical power in the two branches was approximately 9:1 (switching ratio 9.5 dB). We calculated a total insertion loss of the waveguide to be less than 1 dB, however, there are known numerical errors with the standard beam propagation method for angled structures such as ours, and we suspect that these cause the loss to be underestimated. We are developing more accurate wide angle beam propagation algorithms in order to more accurately predict the loss in our device.[15]

Typical results of simulations of the time dependence of the device are shown in figure 5 for the same switch geometry and applied heater power. The ratio reaches a maximum near 1.0 ms, followed by a slight decrease, which is due to the temperature profile becoming more homogeneous with time. Increasing the applied heater power does not

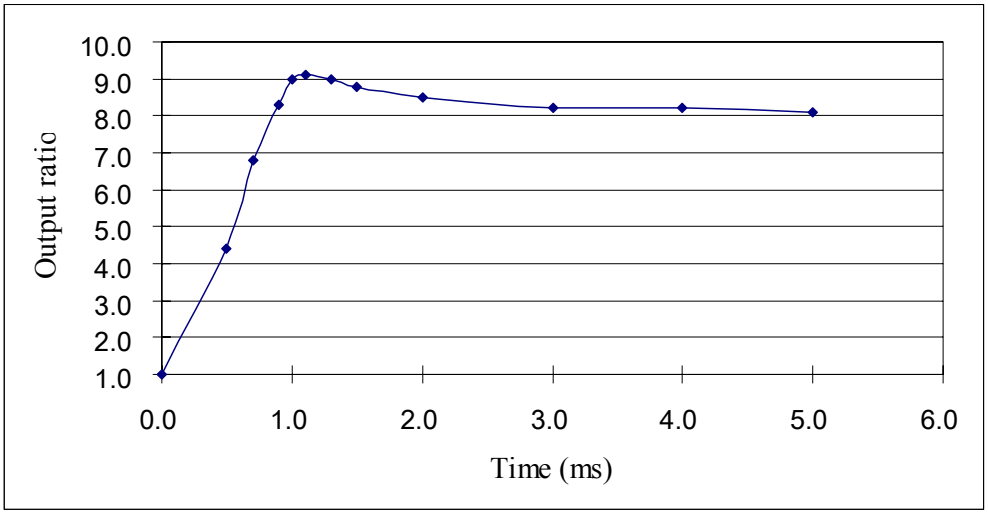

Figure 5: Plot of the ratio of the power through the output branches as a function of time after application of a heater power of 70 mW.

improve on the switching time; while the temperature increase faster and to a higher value, the gradient does not increase appreciably. The temperature difference across the waveguide for the 70 mW heater power was approximately 25º C, with a maximum of 47º C just above the active heater. At higher temperatures the chance of thermal damage to the device becomes more likely.

2.3. Fabrication and device characterization

The devices were fabricated on glass substrates. The non-Manhattan geometry of the heaters and branch required photolithography masks to be fabricated using electron-beam lithography (University of Alberta nano-fabrication facility). The microheaters consisted of a 300 Å Cr adhesion layer over which a 0.5 μm layer of Au was deposited. The small sizes of both the waveguides and the heaters made the metal etching a delicate process. Optimum adhesion of the metal and good etching was obtained with a 2:1 DI water to Transene TFS (Au) etchant, and a very gentle etching process. The standard procedure had been to agitate the sample during etching, but we found that this caused side-etching problems which eventually destroyed the narrow heaters. Instead, the sample was left in the etchant for 1 minute intervals without any agitation, rinsed, and then examined under the microscope to determine whether further etching was needed. Following the Au etch, the Cr adhesion layer was also removed by etching.

The deposited Au microheaters are shown in figure 6. The dimensions are the same as those shown in figure 3. The measured resistance of the heaters ranged from 60 to 160 Ω, depending on the length of the serpentine element. These values include contact resistance between the probes and contact pads, and values are consistent with theoretically calculated values for the given Au film thickness and width.

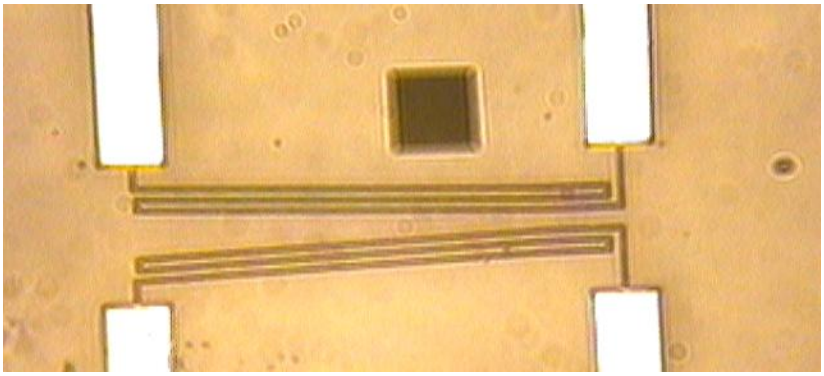

Figure 6: Au microheaters. The dark square is an artifact of the camera.

The SU-8 was deposited by spin coating the photoresist onto the dehydrated substrates. A two-step spin cycle was used, the first is a low-speed spread cycle (500 rpm for 10 seconds) immediately followed by a high-speed coat cycle (3000 rpm for 30 seconds). An initial thin layer of SU-8-5 was coated onto the substrate to promote adhesion. SU-8-X indicates a formulation of SU-8 of varying concentration in the solvent gamma butyrolactone, and therefore different viscosity. The "X" denotes the approximate film thickness achieved with a standard spin coating procedure. After spinning on the SU-8-5, the film was soft baked on a level hotplate at 65º C for 1 minute and allowed to cool. Following this, SU-8-25 was spun on and soft-baked at 65º C for 3 minutes, then patterned by exposing the substrates under UV for 3 minutes and 45 seconds using a Karl Suss contact aligner. A post-exposure bake on hot plate at 65º C for 1 minute, then 95º C for 3 minutes fixed the patterned structures in the polymer. The SU-8 was developed in SU-8 developer for 1 minute intervals while checking the device under a microscope to avoid over-developing. One problem we encountered related to adhesion: the waveguides were easily separated from the substrate. We are currently investigating the effect of a blanket cladding layer of poly(dimethylsiloxane) (PDMS) to both protect the waveguides as well as provide a higher index cladding for the upper surfaces.

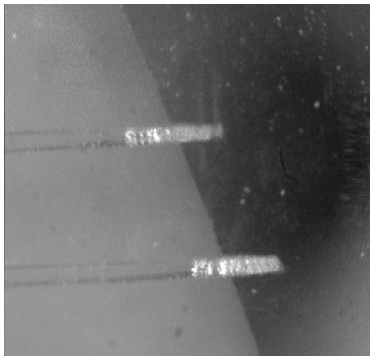

Figure 7: Light emission from the ends of the two arms of the Y-branch for no applied heater power.

Preliminary testing was carried out on the fabricated devices. Light from a HeNe laser was coupled in to the waveguides using prism coupling, with an index matching gel to obtain good optical contact between the prism and waveguide. Figure 7 shows an image of the two output branches of the device with no applied heater power. The light emitted from the ends is approximately equal, although a quantitative measurement of the power has not yet been performed. Measurement of the output power ratio will be accomplished by cleaving the output branch ends of the waveguide in order to obtain reasonably good optical quality, then imaging the emission from the fibers end on with a CCD camera.

3. CONCLUSION

Simulations of the switching behavior were presented for a novel thermooptic switch which uses an inhomogeneous refractive index gradient to guide light into one of two output channels. Preliminary optimization of the device geometry and operation parameters resulted in simulated switching times of 1 ms with an applied heater power of 70 mW. The device was fabricated and initial characterization of the switch has confirmed waveguiding through the Y-branch to the output. The completed device will be novel in using a refractive index gradient to actively steer the beam, as well as the use of a single polymer material as waveguide and active switching material, allowing simple fabrication of the waveguide structure in a single processing step.

4. ACKNOWLEDGEMENT

This material is based upon work partially supported by the National Science Foundation under Grant No. 0348955.

5. REFERENCES

1. M. Bourouha, M. Bataineh, M. Guizani, “Advances in Optical Switching and Networking: Past, Present and Future” 405-413, Proc. of IEEE SoutheastCon, Columbia, SC, 2002.
2. S. Oktyabrsky, J. Castracane, A. Kaloyeros, “Emerging Technologies for Chip-Level Optical Interconnects” Proc. of the SPIE **4652**, 213-224, 2002.
3. R. Baets, L. Vanwassenhove, “2D inter-chip optical interconnects” Opt. Mater. **17,** 227-233, 2001.
4. K. Okamoto, “PLC Technologies: Present and Future” Proc. of the SPIE **4532**, 86-92, 2001.
5. J. Thackera, J. Chon, G. Bjorklund, W. Volksen, D. Burland, “Polymeric electro-optic Mach-Zehnder Switches” Appl. Phys. Lett. **67**, 3874-76, 1995.
6. M. Kawachi, “Silica-Based Planar Lightwave Circuit Technologies” *Proc. IOOC-ECOC '91 : 17th European Conference on Optical Communication*, pp. 51-58, 1991.
7. T. Kaino, I. Yokohama, S. Tomaru, M. Amano, M. Hikita, “Development of Polymer Optical Waveguides for Photonic Device Applications” in *ACS Symp. Series 672 Photonic and Optoelectronic Polymers*, S Jenekhe, K. Wynne Eds., pp. 30-46, 1997.
8. L. Eldada, L. Shacklette, “Advances in Polymer Integrated Optics” IEEE J. Sel. Topics Quant. Elec. **6**, 54-68, 2000.
9. G.B. Lee, C.H. Lin, G.L. Chang, “Multi-Cell-Line Micro Flow Cytometers with Buried SU-8/SOG Optical Waveguides” *MEMS 2002 Tech. Digest,* 503-503, Las Vegas, NV, 2002.
10. D. B. Miller, "Rationale and challenges for optical interconnects to electronic chips", Proc. of the IEEE **88**, 728-749, 2000.
11. C. Ma, E. Van Keuren, "Simulations of thermo-optic effect in beam propagation" Proc. of the SPIE **5595**, 394-403, 2004.
12. C. Ma, E. Van Keuren, "New design of a beam-steering thermooptic multimode polymer waveguide switch" Appl. Phys. B: Lasers and Optics, in press.
13. R. Scarmozzino, B. Whitlock, E. Heller, R. Osgood, “Numerical methods for modeling photonic devices and systems” Proc of the SPIE, **3944**, 548-60 2000.
14. S-T. Chu, W-P. Huang, S-K. Chaudhuri, “Simulation and analysis of waveguide based optical integrated circuits” Comp. Phys. Comm. **68**, 451-84, 1991.
15. C. Ma, E. Van Keuren, “A simple three dimensional wide-angle beam propagation method”, *Optics Express*, **14**, 4668-4674, 2006.